Pharmaceutical Research

# 'IN VITRO', 'IN VIVO' AND 'IN SILICO' INVESTIGATION OF THE ANTICANCER EFFECTIVENESS OF OXYGEN-LOADED CHITOSAN-SHELLED NANODROPLETS AS POTENTIAL DRUG VECTOR

--Manuscript Draft--

| | |
|---|---|
| **Manuscript Number:** | PHAM-D-17-00365R2 |
| **Article Type:** | Original Article |
| **Full Title:** | 'IN VITRO', 'IN VIVO' AND 'IN SILICO' INVESTIGATION OF THE ANTICANCER EFFECTIVENESS OF OXYGEN-LOADED CHITOSAN-SHELLED NANODROPLETS AS POTENTIAL DRUG VECTOR |
| **Short Title:** | INVESTIGATION OF EFFECTIVENESS OF NANODROPLETS AS DRUG VECTOR |
| **Corresponding Author:** | Ilaria Stura<br>Università degli Studi di Torino<br>Torino, Piemonte ITALY |
| **Corresponding Author's Institution:** | Università degli Studi di Torino |
| **Order of Authors:** | Amina Khadjavi |
| | Ilaria Stura |
| | Mauro Prato |
| | Valerio Giacomo Minero |
| | Alice Panariti |
| | Ilaria Rivolta |
| | Giulia Rossana Gulino |
| | Federica Bessone |
| | Giuliana Giribaldi |
| | Elena Quaglino |
| | Roberta Cavalli |
| | Federica Cavallo |
| | Caterina Guiot |
| **Section/Category:** | Drug delivery and targeting |
| **Keywords:** | Chitosan nanodroplet; antitumor nanodevice; nanocarrier; Breast Cancer; oxygen |
| **Funding Information:** | Compagnia di San Paolo (ORTO11CE8R) — Prof Caterina Guiot |
| **Abstract:** | Purpose: Chitosan-shelled/decafluoropentane-cored oxygen-loaded nanodroplets (OLN) are a new class of nanodevices to effectively deliver anti-cancer drugs to tumoral cells. This study investigated their antitumoral effects 'per se', using a mathematical model validated on experimental data.<br>Methods: OLN were prepared and characterized either in vitro or in vivo. TUBO cells, established from a lobular carcinoma of a BALB-neuT mouse, were investigated following 48 h of incubation in the absence/presence of different concentrations of OLN. OLN internalization, cell viability, necrosis, apoptosis, cell cycle and reactive oxygen species (ROS) production were checked as described in the Method section. In vivo tumor growth was evaluated after subcutaneous transplant in BALB/c mice of TUBO cells either without treatment or after 24 h incubation with 10% v/v OLN.<br>Results: OLN showed sizes of about 350 nm and a positive surface charge (45 mV). Dose-dependent TUBO cell death through ROS-triggered apoptosis following OLN internalization was detected. A mathematical model predicting the effects of OLN uptake was validated on both in vitro and in vivo results. |

| | |
|---|---|
| | Conclusion: due to their intrinsic toxicity OLN might be considered an adjuvant tool suitable to deliver their therapeutic cargo intracellularly and may be proposed as promising combined delivery system. |
| **Additional Information:** | |
| **Question** | **Response** |
| Is this manuscript, in any form or version, currently under review elsewhere? If you answer "Yes," please provide an explanation in your cover letter. | No |
| Has this manuscript, in any form or version, previously been rejected by another journal? If you answer "Yes," please provide an explanation in your cover letter. | Yes |
| Has this manuscript, in any form or version, previously been submitted to Pharmaceutical Research? If you answer "Yes," please provide an explanation in your cover letter. If your manuscript was previously rejected, you must include a summary of the revisions you have made. | Yes |
| Do any of the authors of this manuscript have financial disclosures or conflicts of interest to declare? If you answer "Yes," please provide an explanation in the ACKNOWLEDGMENTS & DISCLOSURES section of your manuscript. If you answer "No," you are certifying on behalf of all authors that there are no relevant interests to disclose. | No |
| Would you like to receive the Table of Contents of new issues of Pharmaceutical Research via email? | No |
| **Author Comments:** | Dear Editor,<br>We resubmit the manuscript 'IN VITRO', 'IN VIVO' AND 'IN SILICO' INVESTIGATION OF THE ANTICANCER EFFECTIVENESS OF OXYGEN-LOADED CHITOSAN-SHELLED NANODROPLETS AS POTENTIAL DRUG VECTOR after a careful revision based on the useful and helpful reviewers' observations.<br>In particular, we completely re-drawn Figure 4 and we commented in the text the MTT values.<br><br>Kind regards,<br><br>the authors |

Dear Editor,

We resubmit the manuscript ‘IN VITRO’, ‘IN VIVO’ AND ‘IN SILICO’ INVESTIGATION OF THE ANTICANCER EFFECTIVENESS OF OXYGEN-LOADED CHITOSAN-SHELLED NANODROPLETS AS POTENTIAL DRUG VECTOR after a careful revision based on the useful and helpful reviewers’ observations.

In particular, we completely re-drawn Figure 4 and we commented the MTT values in the text. Moreover, two papers are inserted in bibliography.

The detailed answers to the reviewers’ comments follow.

REVIEWER 3:

According to reviewer’s suggestion, figure 4 was completely modified with an higher quality. The results of MTT test were commented in the manuscript:

“OLN inhibit TUBO cells cell growth

In order to evaluate the OLN effects on cell growth, TUBO cells treated with increasing doses (2.5%, 5%, 10%, 20% and 40% v/v) of OLN aqueous nanosuspensions were monitored for 24, 48 and 72 hours by MTT assay. OLN treatment reduced the viability of TUBO cells in a concentration- and time-dependent manner. Interestingly, no significant inhibition of cell proliferation was observed up to 10%-OLN dose. The highest growth inhibition was reached after 48 hours of treatment with 40% v/v of OLN, which induced approximately a 90% reduction in cell viability respect to controls. On the other hand, the incubation with 20% v/v of OLN induced only about 30% of inhibition of cell viability.
Based on these results, the doses corresponding to 20% and 40% v/v of OLN were not considered for further experiments.”

# 'IN VITRO', 'IN VIVO' AND 'IN SILICO' INVESTIGATION OF THE ANTICANCER EFFECTIVENESS OF OXYGEN-LOADED CHITOSAN-SHELLED NANODROPLETS AS POTENTIAL DRUG VECTOR

Amina Khadjavi[*], Ilaria Stura[*], Mauro Prato[1], Valerio Giacomo Minero[2], Alice Panariti[3], Ilaria Rivolta[3], Giulia Rossana Gulino[4], Federica Bessone[5], Giuliana Giribaldi[4], Elena Quaglino[2], Roberta Cavalli[5], Federica Cavallo[2], Caterina Guiot

*Dipartimento di Neuroscienze, Università di Torino, Torino, Italy*

[1]*Dipartimento di Scienze della Sanità Pubblica e Pediatriche, Università di Torino, Torino, Italy*

[2]*Dipartimento di Biotecnologie Molecolari e Scienze per la Salute, Università di Torino, Torino, Italy*

[3]*Dipartimento di Medicina Sperimentale, Università Milano Bicocca, Monza, Italy*

[4]*Dipartimento di Oncologia, Università di Torino, Torino, Italy*

[5]*Dipartimento di Scienze e Tecnologia del Farmaco, Università di Torino, Torino, Italy*

*** AK & IS EQUALLY CONTRIBUTED TO THE PAPER**

* Corresponding authors: Dr. Ilaria Stura, Dipartimento di Neuroscienze, Università di Torino, Corso Raffaello 30, 10125 Torino, Italy; Phone: +39-011-670-8198; Fax:+39-011-670-8174; e-mail: ilaria.stura@unito.it

**Abstract**

**Purpose**: Chitosan-shelled/decafluoropentane-cored oxygen-loaded nanodroplets (OLN) are a new class of nanodevices to effectively deliver anti-cancer drugs to tumoral cells. This study investigated their antitumoral effects '*per se*', using a mathematical model validated on experimental data.

**Methods**: OLN were prepared and characterized either *in vitro* or *in vivo*. TUBO cells, established from a lobular carcinoma of a BALB-neuT mouse, were investigated following 48 h of incubation in the absence/presence of different concentrations of OLN. OLN internalization, cell viability, necrosis, apoptosis, cell cycle and reactive oxygen species (ROS) production were checked as described in the Method section.

*In vivo* tumor growth was evaluated after subcutaneous transplant in BALB/c mice of TUBO cells either without treatment or after 24 h incubation with 10% v/v OLN.

**Results**: OLN showed sizes of about 350 nm and a positive surface charge (45 mV). Dose-dependent TUBO cell death through ROS-triggered apoptosis following OLN internalization was detected. A mathematical model predicting the effects of OLN uptake was validated on both *in vitro* and *in vivo* results.

**Conclusion**: due to their intrinsic toxicity OLN might be considered an adjuvant tool suitable to deliver their therapeutic cargo intracellularly and may be proposed as promising combined delivery system.

**Keywords:** Chitosan nanodroplet, antitumor nanodevice, nanocarrier, breast cancer, oxygen

**Abbreviations**

DAPI = Diamidino-2-phenylindole dihydrochloride

DMEM = Dulbecco's Modified Eagle Medium

FITC = fluorescein isothiocyanate

LDH= lactate dehydrogenase

MTT = 3-(4,5-dimethylthiazol-2-yl)-2,5-diphenyltetrazolium bromide

OLN = Oxygen-loaded Nanodroplets

ROS = Oxygen Reactive Species

## Introduction

Innovative drug delivery nanodevices can improve the pharmacokinetics and biodistribution of chemoterapeutics (1). Since cells can internalize small materials (2), drug delivery systems at the nanoscale range are expected to provide new interesting therapeutic approaches (3). Nanoparticle sizes are small enough to allow intra- or trans-capillary passage while surface modification can be tuned to avoid macrophage uptake and to favour the accumulation in specific tissues. Nanoparticles, when properly synthesized from biodegradable materials (4), can be biocompatible and improve the stability of active compounds. Furthermore, they can overcome drug resistance issues by greatly improving drug effectiveness and reducing chances for side effects to arise (1, 5). Hypoxia-activated, near-infrared (NIR) light-triggered chitosan nanoparticles have been developed to deliver drugs to cancer cells (6). Recently, a new class of nanodevices for oxygen storage and release has been designed, namely perfluoropentane-based oxygen-loaded nanobubbles and decafluoropentane-based oxygen-loaded nanodroplets (7, 8). Both nanodevices, coated with biocompatible and biodegradable polysaccharides such as dextran sulfate or chitosan, proved to be effective in oxygen delivery either *in vitro* or *in vivo* (7-10). Chitosan-shelled/decafluoropentane-cored oxygen-loaded nanodroplets (OLN), having average diameters of about 700 nm, positive charge and long-term stability (7) have been designed as potential therapeutic tools to promote healing processes in infected chronic wounds, since chitosan-based OLN displayed antimicrobial properties against methylcillin-resistant *Staphylococcus aureus* and *Candida albicans* (11). Interestingly, this types of OLN showed the capability to overcome hypoxia-dependent dysregulation of matrix-associated proteolytic enzymes such as matrix metalloproteinases (12).

In the present study the effects of chitosan-shelled OLN on the growth of TUBO breast cancer cells will be designed either *in vitro* or *in vivo.* OLN internalization by TUBO cells was investigated and its effectiveness on cell viability along with some possible underlying mechanisms was assessed with the aim to define the key parameters. For this purpose, a simple mathematical model

simulating the OLN uptake by TUBO cells and their cell interactions was developed to describe the crucial role played by nanodroplet internalization on the cell viability.

## Materials and Methods

### Materials

Unless otherwise stated, all materials were from Sigma-Aldrich (St Louis, MO). Ethanol (96%) was from Carlo Erba (Milan, Italy); Epikuron 200® (soya phosphatidylcholine 95%) was from Degussa (Hamburg, Germany); palmitic acid, decafluoropentane (DFP), chitosan, and polyvinylpyrrolidone (PVP) were from Fluka (Buchs, Switzerland); ultrapure water was obtained using a 1-800 Millipore system (Molsheim, France); Ultra-Turrax SG215 homogenizer was from IKA (Staufen, Germany); PEN-STREP was from Cambrex Bio Science (Vervies, Belgium); LSM710 inverted confocal laser scanning microscope was from Carl Zeiss (Oberkochen, Germany); Synergy HT microplate reader was from Bio-Tek Instruments (Winooski, VT); FACScan flow cytometer and CellQuest software were from Becton & Dickinson (Mountain View, CA); SPSS 16.0 software from SPSS (Chicago, IL, USA). TUBO cells were kindly provided by Dr. Laura Conti, Molecular Biotechnology Center, University of Torino. BALB/c mice were bred under specific pathogen-free conditions (Allentown Caging Equipment, Allentown, NJ) at the Molecular Biotechnology Center and treated according to current European guidelines and policies. The experimental plan was approved by the Bioethical Committee of the University of Torino.

### Preparation of FITC-labeled chitosan

FITC-labeled chitosan was obtained by the reaction between the isothiocyanate group of FITC and the primary amine group of the d-glucosamine residue of chitosan. For this purpose, one gram of chitosan was dissolved in 100 ml of 0.10 M acetic acid. To the chitosan solution, 100 ml of dehydrated methanol was slowly added with continuous stirring. A FITC methanol solution (2

mg/ml), was slowly added to the chitosan solution. The reaction was allowed to proceed for 3 h in the dark at room temperature. FITC-labeled chitosan was precipitated in 0.1 M sodium hydroxide solution. The precipitate was washed extensively with deionized distilled water, to eliminate free FITC. The labeled polymer was then freeze dried.

**Preparation of chitosan-shelled/decafluoropentane-cored OLN**

Chitosan-shelled/decafluoropentane-cored **(**OLN) were prepared as previously described using a two-step method (7, 8). At first, a decafluoropentane nanoemulsion was obtained and stabilized with dipalmitoylphosphatidylcholine and palmitic acid (1% w/v). The nanoemulsion was saturated with oxygen, up to a gas concentration of 30 mg/L. Subsequently, a chitosan solution (2.7% w/v) at pH = 5.5 was added dropwise under stirring, maintaining the oxygen purge up to 30 mg/L.

Fluorescent-labelled OLN were then prepared with the same preparation protocol above described but using fluorescein isothiocyanate (FITC)-chitosan for the shell.

The two OLN formulations were sterilized through ultraviolet (UV)-C ray exposure for 20 min. To control the sterilization efficacy, UV-C treated OLN were incubated with cell culture DMEM medium in a humidified $CO_2$/air incubator at 37°C up to 72 h. No signs of microbial contamination were observed when OLN and FITC-labeled OLN were checked by optical microscopy.

**Physico-chemical characterization of chitosan-shelled/decafluoropentane-cored OLN**

Blank-unlabelled and fluorescent-labelled OLN formulations were *in vitro* characterized to evaluate size, morphology and surface charge. The average diameter and polydispersity index of the OLN formulations were measured by photocorrelation spectroscopy (PCS) using a 90 Plus instrument (Brookhaven, NY, USA) at a fixed angle of 90° and a temperature of 25 °C after dilution with filtered water. Each value represents the average of five measurements of three different sample batches. For zeta potential determination, the diluted OLN formulations were placed in an electrophoretic cell, where a rounded 15 V/cm electric field was applied. Each value reported is the

average of ten measurements of three different formulations. The morphology of unlabelled-OLN formulations was determined by transmission electron microscopy (TEM) analysis performed using a Philips CM10 instrument (Eindhoven, NL). Nanodroplet preparations were dropped onto a Formvar-coated copper grid and air-dried prior to examination.

### *In vitro* oxygen release from chitosan-shelled/decafluoropentane-cored (OLN)

*In vitro* oxygen release from chitosan-shelled/decafluoropentane-cored OLN was investigated using the dialysis bag technique. The donor phase, consisting of 3 mL of OLN formulation, was placed in a dialysis bag (cellulose membrane, molecular weight of 12–14,000 Da), hermetically sealed and immersed in 45 mL of the receiving phase. The receiving phase consisted of 0.9% (w/v) NaCl (saline) solution whit a oxygen concentration of 4 mg/L. The oxygen concentration was previously reduced with a $N_2$ purge in order to mimic hypoxic conditions. Then, the oxygen release kinetics from OLN was monitored for 8 hours, using an oxymeter (HQ40d model, Hach) at 37 °C.

### Cell cultures

TUBO cells, a cloned rat Her2/neu$^+$ cell line established from a lobular carcinoma of a BALB-neuT mouse (13) were cultured in high glucose DMEM, containing 20% fetal bovine serum (FBS), 2 mM L-glutamine and 1 % penicillin-streptomycin (PEN-STRE TEMP) in a humidified $CO_2$/air-incubator at 37°C.

### Evaluation of OLN uptake by TUBO cells

TUBO cells were plated in 6-well plates on glass coverslips and incubated in DMEM medium for 24 h with/without 10% v/v FITC-labelled OLN in a humidified $CO_2$/air-incubator at 37°C. The procedure followed is fully described in (8).

**Cell viability assay**

Cell viability was checked by MTT assay. Cells were seeded at $4\times10^4$ cells/200 µl of medium per well in 96-well plates. Twenty-four hours after plating, cells were left untreated or treated with various doses of OLN (2.5 %, 5%, 10%, 20%, 40% v/v) up to 72 hours. Thereafter, each well received 5 µl of fresh MTT (5mg/ml in PBS) followed by incubation for 2 hr at 37°C. The supernatant growth medium was removed from the wells and replaced with 100 µl of DMSO to solubilize the dark blue formazan crystals. After 15 minutes of incubation, the absorbance (OD) of the culture plate was read at a wavelength of 562 nm using a Synergy HT microplate reader. Viability of controls was arbitrary fixed to 100%.

**Lactate dehydrogenase (LDH) release measurement**

The potential necrotic effect of OLN was measured as the release of lactate dehydrogenase (LDH) from TUBO cells into the extracellular medium. Briefly, TUBO were seeded $1x10^6$ cells/2 ml of medium per well in 6-well plates. Twenty-four hours after plating, cells were incubated for 48 h in the presence or absence of increasing doses (2.5 %, 5%, and 10% v/v) of OLN at 37°C in a 5 % $CO_2$ atmosphere. The measurement procedure is described in details in (8).

**Hypodiploid peak evaluation and cell cycle phase analysis**

DNA distribution analysis was performed by flow cytometry. Briefly, TUBO were seeded $1x10^6$ cells/2 ml of medium per well in 6-well plates. Twenty-four hours after plating, cells were incubated for 48 h with OLN (2.5 %, 5%, and 10% v/v). Next, TUBO cells were treated as described in (14).

**Reactive Oxygen Species (ROS) detection**

To evaluate ROS production in OLN treated TUBO cells, ROS-mediated fluorescent activation of the compound 5-(and 6)-carboxy-2′-7′-dichlorofluorescein diacetate (carboxy-$H_2$DCFDA; Molecular Probes, Invitrogen) was measured, according to manufacturer's instructions. Briefly, cells

were seeded in black 96-well plates at $4 \times 10^4$ cells/200 µl of medium per well. Twenty-four hours after plating, cells were treated with increasing doses of OLN (2.5 %, 5%, and 10% v/v) for 24 hours. Then, cells were supplied with carboxy-$H_2$DCFDA (10 µM) in phenol red–free DMEM for 1 hour, washed and incubated in phenol red–free DMEM without carboxy-$H_2$DCFDA. Treatment with $H_2O_2$ (100 µM) was used as positive control. ROS generation was measured using a fluorescence plate reader ($\lambda_{ex}$=485 nm, $\lambda_{em}$=535 nm) using a Synergy HT microplate reader. ROS control value was arbitrary fixed to 1. Data are expressed as fold increase compared to untreated control.

***In vivo* experiments**

Ten-week-old BALB/c female mice were challenged subcutaneously in the left flank with $1x10^5$ TUBO cells diluted in 200 µl of PBS (control, *n*=5) or with $1x10^5$ TUBO cells and 10% v/v OLN suspension in PBS (*n*=5). The mammary fat pads of all mice were inspected and palpated twice a week for tumor appearance and growing masses > 1 mm in mean diameter were regarded as tumors. Individual neoplastic masses were measured with calipers in 2 perpendicular diameters X and Y. Tumor mean diameter was calculated as (X+Y) / 2, and values computed on 5 mice are reported as mean ± SEM. Mice were sacrificed when one tumor exceeded a 10-mm mean diameter. All procedures were done in accordance with the EU guidelines and policies and with the approval of the University of Torino animal care committee (16/03/2011).

**Statistical analysis**

Data from MTT assay, LDH measurement, flow cytometry and ROS evaluation are expressed as the mean±standard deviation (SD) from three independent experiments analyzed in triplicate. Data from confocal microscopy are representative images from three independent experiments with similar results analyzed in duplicate. Statistical differences among different groups were determined

by one-way analysis of variance (ANOVA) using SPSS 16.0 software (SPSS, Chicago, IL, USA). P values (*p*) less than 0.05 were considered as statistically significant.

**Mathematical model**

The simulation of the cellular uptake of nanoparticles has been tackled by Salvati and colleagues (15) in 2011 and the toxicity has been evaluated by Maher and collegues (16) in 2014. More recently, (17) Souto *et a*l. proposed a model for simulating the localization of doxorubicin loaded chitosan particles in cells from which we took inspiration for the design of a simplified compartmental model.

Based on experimental results, we hypothesized that:

- OLN are internalized only by a fraction of total TUBO cells (possibly in a dose-dependent manner);

- TUBO cells, which do not internalize OLN, duplicate with a rate $\lambda = \ln(2)/T$ which can be deduced by the experimental duplication time T= 36 hours. They represent the Vital (V) population.

- in the other cell population, OLN, after internalization, interact with some intracellular ROS generating mechanism, which may induce, after a time delay, named t0 and related to the uptake time, some apoptotic phenomena.

Toxicity decays from TOX (possibly dose dependent) to 0 with rate m (possibly related to the growth rate as $m=k\lambda$). For $t < t0$ all cells belong to V and duplicate with rate $\lambda$.

-After t0 an Apoptotic (A) population develops constituted by the V cells which are unable to duplicate. However, when $t >> t0$ the A cells population disappears with a death rate $\mu$.

$$\frac{dV}{dt} = \lambda V - TOX(d)\, e^{-m(t-t_0)} V \qquad (1)$$

$$\frac{dA}{dt} = TOX(d)\, e^{-m(t-t_0)} V - \mu A \qquad (2)$$

Both cell populations contribute to the MTT measured at different times:

$$MTT = \frac{V}{V + A} \qquad (3)$$

Eqns(1-3) can be solved numerically but some information can be obtained by experimental results In particular, two states of equilibrium are predictable. In the first one, i.e. when $\lambda \leq TOX(d) \exp(-m(t-to))$, the OLN treatment is very effective, cell regrowth is prevented and both cell populations disappear. On the other hand, i.e. when $\lambda > TOX(d) \exp(-m(t-to))$, the V cells population is restricted only for a limited time and cells regrowth is expected after a (OLN dose-dependent) time delay.

## Experimental results

### Physico-chemical characterization of chitosan-shelled/decafluoropentane-cored OLN

The results of the physico-chemical characterization of chitosan-shelled/decafluoropentane-cored OLN are reported in the Table I.

TEM image of Blank OLN showed the spherical shape and a well-defined core-shell structure of nanodroplets (Fig. 1). The physico-chemical characteristics of Fluorescent-labelled OLN did not change.

[Insert Fig. 1]

### *In vitro* oxygen release from chitosan-shelled/decafluoropentane-cored OLN

OLN ability to store and release oxygen was *in vitro* evaluated. Fig. 2 shows the percentage of the oxygen released from OLN in a hypoxic receiving chamber over time up to 8 hours. Results are shown as fold change of oxygen released relative to the initial concentration of 30 mg/L of the suspension.

[Insert Fig. 2]

Not burst effect was observed. This behavior proved that oxygen is released by a diffusion mechanism from the internal core of the OLN.

**OLN internalization in TUBO breast cancer cells**

To study the ability of TUBO cells to internalize OLN, a confocal analysis was performed. TUBO cells were incubated for 24 hours with OLN shelled with FITC-labeled chitosan. After fixation and staining with DAPI, confocal microscopy images showed that florescent-labelled OLN were avidly and fast internalized by TUBO cells (Fig. 3).

The CLSM analyses demonstrated the OLN internalization of Fluorescent-labelled OLN in TUBO cells.

[Insert Fig. 3]

**OLN inhibit TUBO cells cell growth**

In order to evaluate the OLN effects on cell growth, TUBO cells treated with increasing doses (2.5%, 5%, 10%, 20% and 40% v/v) of OLN aqueous nanosuspensions were monitored for 24, 48 and 72 hours by MTT assay. OLN treatment reduced the viability of TUBO cells in a concentration- and time-dependent manner. Interestingly, no significant inhibition of cell proliferation was observed up to 10%-OLN dose. The highest growth inhibition was reached after 48 hours of treatment with 40% v/v of OLN, which induced approximately a 90% reduction in cell viability respect to controls. On the other hand, the incubation with 20% v/v of OLN induced only about 30% of inhibition of cell viability.

Based on these results, the doses corresponding to 20% and 40% v/v of OLN were not considered for further experiments.

[Insert Fig. 4]

**OLN promote apoptosis- but not necrosis-related TUBO cell death**

The effect on apoptosis and necrosis of increasing doses of OLN (2.5 %, 5%, 10% v/v) when incubated for 48 h with TUBO cells were measured as alternative parameters of cell death by LDH assay and flow cytometry, respectively (Fig. 4). As shown in panel 4A, no differences in the percentage of necrosis between OLN-treated (all doses) and untreated TUBO cells were observed. On the other hand, as shown in panels 4B, OLN promoted cell apoptosis, thus increasing the hypodiploid cell peak, in a dose-dependent manner, with ~80% cell apoptosis being detected at the highest dose of OLN.

**Evaluation of OLN effects on TUBO cell cycle**

OLN effects on cell cycle distribution were investigated by flow cytometry. DNA content was measured in TUBO cells after being left untreated or treated with increasing doses (2.5 %, 5%, 10% v/v) of OLN nanosuspension for 48 hours. As shown in Fig. 4C, OLN did not cause any differences compared to controls in none of TUBO cell cycle phases (S, G0/G1, and G2/M).

**OLN induce ROS generation in a dose-dependent manner**

After *in vitro* treating TUBO cells with increasing doses of OLN nanosuspension (2.5 %, 5%, 10% v/v) for 24 hours, ROS generation was assessed by measuring the fluorescent activation of carboxy-$H_2$DCFDA. As shown in Fig. 4D, OLN enhanced ROS production with respect to untreated cells in a dose-dependent manner, reaching a 40% ROS increase at the highest dose.

**Evaluation of OLN effects on *in vivo* TUBO tumor growth**

An *in vivo* experiment was carried out to obtain the proof of concept of the OLN activity on mice tumor growth. From the preliminary results it seems that OLN might be able to affect tumor growth.

Indeed, when 10-week-old BALB/c female mice were challenged subcutaneously into the mammary fat pad with TUBO cells without OLN, a progressively growing tumor appeared in all mice.

On the other hand, the results were different with OLN. Also it is necessary to take into account that high variability in tumor growth was observed when TUBO cells were inoculated in the presence of OLN. In two out of five mice TUBO cells did not grow, whereas in other two animals the tumor growth appeared strictly delayed. Only in one case the tumor growth rate was similar to that observed in the control group (Fig. 5). This is an explorative *in vivo* experiment and more animals would be necessary to draw a conclusion. These data can be used for the validation of the mathematical model.

[Insert Fig. 5]

**Modelling results**

*a.* *In vitro* cells viability

Fig. 6 reports the comparison between the MTT measured results for the 4 different studied doses of OLN and the model predictions. The parameter values were selected as: $\lambda$= 0.019 1/h; m=0.1 1/h (k=5.26), $\mu$=0.001 1/h, TOX(10uM**)** = 0.20; TOX(20uM) = 0.22; TOX(40uM) = 0.25; TOX(80uM) = 0.39.

[Insert Fig. 6]

*b.* *In vivo* cell viability

Fig. 7 reports the measurements (mean ± SEM) of the control group (blue line) and of the mice treated with OLN (exp=red points, model simulation=line). It is well evident that, after OLN treatment, the tumor growth is impaired with respect to the control (the red points were below the

blue line), and the model (black dotted line) seems able to interpolate the experimental data using the parameter values validated on the *in vitro* model (and not fitting values selected *ad hoc*). The passage from diameter (mm) to number of cells was performed according to the assumption that 1 mm^3 = 10^6 cells.

[Insert Fig. 7]

Starting from the value estimated from the control group (λ=0.0096 1/h), simulations were performed using the same values for k, μ and TOX (20 μM) used for the *in vitro* model.

Taking into account the tumor growth it is always reduced by OLN: it has been significantly slowed in two mice and completely stopped in other two mice. The curve predicted by the numerical simulation, which assumes the same parameter values of the *in-vitro* model, fits well with the experimental results and could easily be applied to reproduce each experimental dataset by properly adapting the parameter values.

**Discussion**

Much research has led to the development of nanodevices with antitumor effects and/or capability to selectively deliver drugs to targeted tissues, thus reducing side effects and improve drug effectiveness (18). The design of nanostructures able to overcome the biological barriers and to affect the uptake within cells have been deeply investigated (19). The *in vivo* nanoparticle fate mainly depends on the morphology, size, surface charge and chemical composition; it might be described using similar models, helpful tool to study and to optimize promising nanoplatforms for drug delivery.

Here, chitosan shelled OLN were selected as model nanocarrier for the design of a model useful for predictive information on nanoparticle uptake behaviour. Chitosan, a positively charged natural

polymer (20, 21), showed interesting physical and biological properties for the preparation of drug delivery systems. Moreover, the cytotoxicity of chitosan and its derivatives toward tumor cells has been reported by several authors (22-28). Interestingly, cationic chitosan nanoparticles have been already exploited as effective nanocarriers due to their ability to be easily internalized by different cell types (29-31). Previously, our group prepared 5-fluorouracil-loaded chitosan nanoparticles, able to increase the cytotoxicity of the drug *in vitro* (32). OLN, comprising 2H,3Hdecafluoropentane core, represent an innovative nanodevice developed using chitosan as shell component. As the present study shows, OLN were significantly internalized *in vitro* by TUBO breast cancer cells, inducing a high cytotoxic activity on this cell line. The OLN uptake by tumor cells can be described as a twostep process, comprising firstly their binding on the cell membrane by electrostatic interactions (33) and their subsequent internalization. As previously demonstrated, the larger the zeta potential of the nanoparticles, the stronger the interactions with tumor cell membrane, favouring the internalization and leading to more severe cytotoxicity. The cationic chitosan can remarkably affects the cell uptake since the positively charged amino groups of chitosan can establish electrostatic interactions with the negatively charged groups exposed on the membrane of tumor cells (34). Therefore, the high surface charge of about 45 mV of OLN might appear a likely cause for their cytotoxic activity. Several studies have demonstrated that chitosan can induce cell death by promoting necrosis (22, 23) or by inducing apoptosis (27, 28) depending on cancer cell type. Cells undergoing apoptosis express cell surface molecules which promote their removal by neighbouring phagocytes. On the other hand, necrotic cells are not generally removed as intact cells and their degradation often causes inflammation (35). OLN appear to exert *per se* a cytotoxic activity on TUBO cells *in vitro* by inducing apoptosis, but not necrosis, mediated cell death. They are, therefore, likely to avoid the triggering of the inflammatory responses.

OLN did not affect the cell cycle kinetics of TUBO cells. However, OLN induced an increase of ROS levels. Various studies showed that ROS can be produced in different cell compartments and are able to damage by oxidation proteins, lipids and DNA (36, 37). Nanoparticles can induce

physico-chemical oxidative stress in mammalian cells by unbalancing the cellular ROS production over the cellular antioxidant defenses through mechanisms still not completely known.

The critical role of ROS in nanoparticle-mediated cytotoxicity and genotoxicity has been reported by several researchers (38-42). The molecular oxygen content of OLN did not produce singlet oxygen. The oxidation capability of OLN was evaluated using a lipo-peroxidation assay on linolenic acid, incorporated in liposomes to mimic the membrane phospholipid bilayer. After the exposure to OLN the linolenic acid did not underwent to lipid peroxidation. Indeed, the oxygen loaded within OLN was not able to induce a direct lipo-peroxidation (data not shown). These results are in line with the previous data reported by Magnetto et al (7).

The oxygen content of the OLN might affect apoptotic effect with a different mechanism.

A hypothesis to explain oxygen toxicity might be related to the partial pressure increase of oxygen inside the tumor cells (43).

As a matter of fact, oxygen toxicity was detected in case of hyperoxia (e.g. larger fraction of inspired oxygen) at atmospheric pressure or in hyperbaric conditions. The slow diffusion of oxygen from the OLN, together with its low solubility in the intracellular fluid both in-vitro and in-vivo prevents any even transitory condition of hyperoxia.

More than oxygen itself, the interaction of the internalized OLN within the cells may affect mitochondrial respiration, alter the endoplasmatic reticulum activity and also the plasma membrane with its enzyme complexes, including NADPH oxidases or finally activate immune cells. All the above mechanisms can lead to the production of free radicals and be therefore responsible for the toxic effects.

Based on these results OLN might be considered an adjuvant for combination therapy.

The proposed mathematical model, which accounts for the internalization of OLN into the TUBO cells and the subsequent induction of toxicity, satisfactorily explain the experimental *in vitro* and *in vivo* results and shows once again that a nanoparticle effective uptake from cells plays a crucial role and should be promoted or enhanced *in vivo* by proper targeting approaches.

**Conclusions**

In this study we validate a computational models predicting the effects of OLN on the *in vitro* and *in vivo* growth of TUBO breast cancer cells after investigating OLN cellular internalization, cytotoxicity, antitumor efficacy, and the underlying biological mechanisms. Such a model may have many useful applications, since in the last years nanotechnology formulations have been extensively explored looking forward new possible treatments for several diseases, including cancer.

**Acknowledgements**

We gratefully acknowledge Compagnia di San Paolo (Ateneo-San Paolo 2011 ORTO11CE8R grant to CG and MP) and Università di Torino (ex-60% 2013 intramural funds to GG and MP) for funding support to this work. MP holds a professorship granted by Università degli Studi di Torino and Azienda Sanitaria Locale-19 (ASL-19). Thanks are due to Adriano Troia, Chiara Magnetto and Monica Argenziano for suggestions on nanodroplet manufacturing. The authors have no conflicting financial interests.

## Tables

*Table I*

| Average diameter ± SD [nm] | PDI | Z-potential ± SD [mV] | pH |
|---|---|---|---|
| 379.25 ± 34.4 | 0.289 | 45.39 ± 1.02 | 5.00 |

*Physico-chemical characterization of the Blank chitosan-shelled/decafluoropentane-cored OLN formulations. Each point represents the mean ± SD of four different formulations (n=4).*

**Figure legends**

**Figure 1. TEM image of OLN (magnification 39,000×).** Scale bar, 300 nm.

**Figure 2. *In vitro* oxygen release from OLN formulations over time measured by an oximeter.** Mean (± S.D.) of the relative (fold change) % oxygen released from OLN of four different formulations (n=4).

**Figure 3. OLN internalization by TUBO cells.**

TUBO cells were untreated (upper panels, Control) or treated with 10 % v/v FITC-labeled OLN (lower panels) for 24 h. After DAPI staining, cells were checked by confocal microscopy. Results are shown as representative images from three independent experiments. Left panels: cell nuclei after DAPI staining (blue). Central panels: FITC-labeled OLN (green). Right panels: merged images. Magnification: 63X.

**Figure 4.**

**A_Analysis of OLN-induced necrosis on TUBO cells.** TUBO cells were untreated or treated with increasing doses of OLN (2.5 %, 5%, 10% v/v) for 48 hours. The percentage of necrotic cells was measured by LDH assay. Results are shown as means±SD from three independent experiments.

**B_ Analysis of OLN induced cell death on TUBO cells.** TUBO cells were untreated or treated with increasing doses of OLN (2.5 %, 5%, 10% v/v) for 48 hours. Apoptosis was assessed by evaluating the accumulation of hypodiploid cells, characterized by a subG1 DNA fluorescence. The percentage of hypodiploid cells was measured by flow cytometry assay. Results are shown as means±SD from three independent experiments. Significance of the differences *vs* untreated cells (0% v/v OLN): ** $p<0.005$;*** $p<0.001$.

**C_ Cell Cycle results.** OLN did not cause any differences compared to controls in none of TUBO cell cycle phases (S, G0/G1, and G2/M).

**D_ OLN effects on TUBO cell cycle distribution.** TUBO cells were untreated or treated with increasing doses of OLN (2.5 %, 5%, 10% v/v) for 48 hours. OLN-effects on cell cycle distribution were investigated measuring by flow cytometry the DNA content in S, G0/G1, and G2/M cell cycle phases. Data are presented as percentage of live cells in single cell cycle phases.

**E_ OLN induced ROS in TUBO cells.** TUBO cells were untreated or treated with increasing doses of OLN (2.5 %, 5%, 10% v/v) for 24 hours. ROS generation was assessed by measurements of fluorescent activation of carboxy-$H_2$DCFDA. ROS control value was arbitrary fixed to 1. Data are means+SD expressed as fold increase compared to untreated control. Significance of the differences *vs* untreated cells (0% v/v OLN): * $p<0.01$; ** $p<0.005$.

**Figure 5. Antitumor response elicited in BALB/c mice by OLN.** The protection was evaluated against TUBO cells in the absence (Ctrl, solid lines n=5) or in the presence (OLN, dotted lines, n=5) of 10% v/v c-OLN. Each line refers to an individual tumor.

**Figure 6. *In vitro*_experimental results of MTT.** MTT evaluated (points) and simulated (lines) after 24, 48 and 72 hrs at 4 different concentrations (2.5 %, 5%, 10%, 20% v/v).

**Figure 7. *In vivo* data.** Tumor growth in control mice and after OLN 10% v/v administration experimental evaluated (blue line for control group and red points for treated mice) compared to model simulated data (dotted lines) using the parameter values validated on the *in vitro* model.

**References**


1. Talevi, A. et al. Applications of nanosystems to anticancer drug therapy (Part I. Nanogels, nanospheres, nanocapsules). Recent patents on anti-cancer drug discovery 2014; 9 (1): 83-98.

2. Ferrari, M. Nanovector therapeutics. Current opinion in chemical biology 2005; 9 (4): 343-6.

3. Gao, H. et al. Mechanics of receptor-mediated endocytosis. Proceedings of the National Academy of Sciences of the United States of America 2005; 102 (27): 9469-74.

4. Mora-Huertas, C.E. et al. Polymer-based nanocapsules for drug delivery. International journal of pharmaceutics 2010; 385 (1-2): 113-42.

5. Barrera, G. et al. Drug Delivery Nanoparticles in Treating Chemoresistant Tumor Cells. Curr Med Chem 2017; 24(42):4800-4815.

6. Lin, Q. et al. Highly discriminating photorelease of anticancer drugs based on hypoxia activatable phototrigger conjugated chitosan nanoparticles. Adv Mater 2013; 25 (14):1981-6.

7. Magnetto, C. et al. Ultrasound-activated decafluoropentane-cored and chitosan-shelled nanodroplets for oxygen delivery to hypoxic cutaneous tissues. Rsc Advances 2014; 4 (72):38433-38441.

8. Prato, M. et al. 2H,3H-decafluoropentane-based nanodroplets: new perspectives for oxygen delivery to hypoxic cutaneous tissues. PLoS One 2015: 10 (3), e0119769.

9. Cavalli, R. et al. Preparation and characterization of dextran nanobubbles for oxygen delivery. Int J Pharm 2009; 381 (2):160-5.

10. Cavalli, R. et al. Ultrasound-mediated oxygen delivery from chitosan nanobubbles. Int J Pharm 2009; 378 (1-2):215-7.

11. Banche, G. et al. Antimicrobial chitosan nanodroplets: new insights for ultrasound-mediated adjuvant treatment of skin infection. Future Microbiol 2015; 10 (6):929-39.

12. Khadjavi, A. et al. Chitosan-shelled oxygen-loaded nanodroplets abrogate hypoxia dysregulation of human keratinocyte gelatinases and inhibitors: New insights for chronic wound healing. Toxicol Appl Pharmacol 2015; 286 (3):198-206.

13. Rovero, S. et al. DNA vaccination against rat her-2/Neu p185 more effectively inhibits carcinogenesis than transplantable carcinomas in transgenic BALB/c mice. J Immunol 2000; 165 (9): 5133-42.

14. Minero, V.G. et al. JNK activation is required for TNFalpha-induced apoptosis in human hepatocarcinoma cells. Int Immunopharmacol 2013; 17 (1):92-8.

15. Salvati, A. et al. Experimental and theoretical comparison of intracellular import of polymeric nanoparticles and small molecules: toward models of uptake kinetics. Nanomedicine 2011; 7 (6):818-26.

16. Maher, M.A. et al. Numerical simulations of in vitro nanoparticle toxicity - the case of poly(amido amine) dendrimers. Toxicol In Vitro 2014; 28 (8):1449-60.

17. Souto, G.D. et al. Evaluation of cytotoxicity profile and intracellular localisation of doxorubicin-loaded chitosan nanoparticles. Anal Bioanal Chem 2016; 408 (20):5443-55.

18. Kanapathipillai, M. et al. Nanoparticle targeting of anti-cancer drugs that alter intracellular signaling or influence the tumor microenvironment. Adv Drug Deliv Rev 2014; 79-80:107-18.

19. Duchene, D. et al. Cyclodextrin-based polymeric nanoparticles as efficient carriers for anticancer drugs. Curr Pharm Biotechnol 2016; 17(3):248-255.

20. Li, Q. et al. Applications and Properties of Chitosan. Journal of Bioactive and Compatible Polymers 1992; 7 (4):370-397.

21. Kumar, M.N.V.R. et al. Chitosan chemistry and pharmaceutical perspectives. Chemical Reviews 2004; 104 (12):6017-6084.

22. Qi, L.F. et al. In vitro effects of chitosan nanoparticles on proliferation of human gastric carcinoma cell line MGC803 cells. World Journal of Gastroenterology 2005; 11 (33):5136-5141.

23. Qi, L.F. and Xu, Z.R. In vivo antitumor activity of chitosan nanoparticles. Bioorganic & Medicinal Chemistry Letters 2006; 16 (16):4243-4245.

24. Jiang, M. et al. Chitosan Derivatives Inhibit Cell Proliferation and Induce Apoptosis in Breast Cancer Cells. Anticancer Research 2011; 31 (4):1321-1328.

25. Salah, R. et al. Anticancer activity of chemically prepared shrimp low molecular weight chitin evaluation with the human monocyte leukaemia cell line, THP-1. International Journal of Biological Macromolecules 2013; 52:333-339.

26. Xu, Y.L. et al. Chitosan Nanoparticles Inhibit the Growth of Human Hepatocellular Carcinoma Xenografts through an Antiangiogenic Mechanism. Anticancer Research 2009; 29 (12):5103-5109.

27. Hasegawa, M. et al. Chitosan induces apoptosis via caspase-3 activation in bladder tumor cells. Japanese Journal of Cancer Research 2001; 92 (4):459-466.

28. Takimoto, H. et al. Proapoptotic effect of a dietary supplement: water soluble chitosan activates caspase-8 and modulating death receptor expression. Drug Metab Pharmacokinet 2004; 19 (1): 76-82.

29. Amidi, M. et al. Chitosan-based delivery systems for protein therapeutics and antigens. Adv Drug Deliv Rev 2010; 62 (1):59-82.

30. Kean, T. and Thanou, M. Biodegradation, biodistribution and toxicity of chitosan. Adv Drug Deliv Rev 2010; 62 (1):3-11.

31. Cavalli, R. et al. New chitosan nanospheres for the delivery of 5-fluorouracil: preparation, characterization and in vitro studies. Curr Drug Deliv 2014; 11(2):270-8.

32. Cavalli, R. et al. New chitosan nanospheres for the delivery of 5-fluorouracil: Preparation, characterization and in vitro studies. Curr Drug Deliv 2014; 11(2):270-278.

33. Wilhelm, C. et al. Intracellular uptake of anionic superparamagnetic nanoparticles as a function of their surface coating. Biomaterials 2003; 24 (6):1001-11.

34. Lee, J.K. et al. Cytotoxic activity of aminoderivatized cationic chitosan derivatives. Bioorg Med Chem Lett 2002; 12 (20):2949-51.

35. Edinger, A.L. and Thompson, C.B. Death by design: apoptosis, necrosis and autophagy. Curr Opin Cell Biol 2004; 16 (6):663-9.

36. Görlach, A. et al. Reactive oxygen species, nutrition, hypoxia and diseases: Problems solved?. Redox biology 2015; 6:372-385.

37. Dunn, J.D. et al. Reactive oxygen species and mitochondria: A nexus of cellular homeostasis. Redox biology 2015; 6:472-485.

38. Hsin, Y.H. et al. The apoptotic effect of nanosilver is mediated by a ROS- and JNK-dependent mechanism involving the mitochondrial pathway in NIH3T3 cells. Toxicol Lett 2008; 179 (3): 130-9.

39. AshaRani, P.V. et al. Cytotoxicity and genotoxicity of silver nanoparticles in human cells. ACS Nano 2009; 3 (2):279-90.

40. Hussain, S.M. et al. In vitro toxicity of nanoparticles in BRL 3A rat liver cells. Toxicol In Vitro 2005; 19 (7):975-83.

41. Limbach, L.K. et al. Exposure of engineered nanoparticles to human lung epithelial cells: influence of chemical composition and catalytic activity on oxidative stress. Environ Sci Technol 2007; 41 (11):4158-63.

42. Park, E.J. et al. Oxidative stress induced by cerium oxide nanoparticles in cultured BEAS-2B cells. Toxicology 2008; 245 (1-2):90-100.

43. Kehrer, J.P. and Klotz, L. Free radicals and related reactive species as mediators of tissue injury and disease: implications for Health. Crit Rev Tox 2015; 45(9): 765-798.

Figure 1

Click here to download Figure Figure 1.jpg

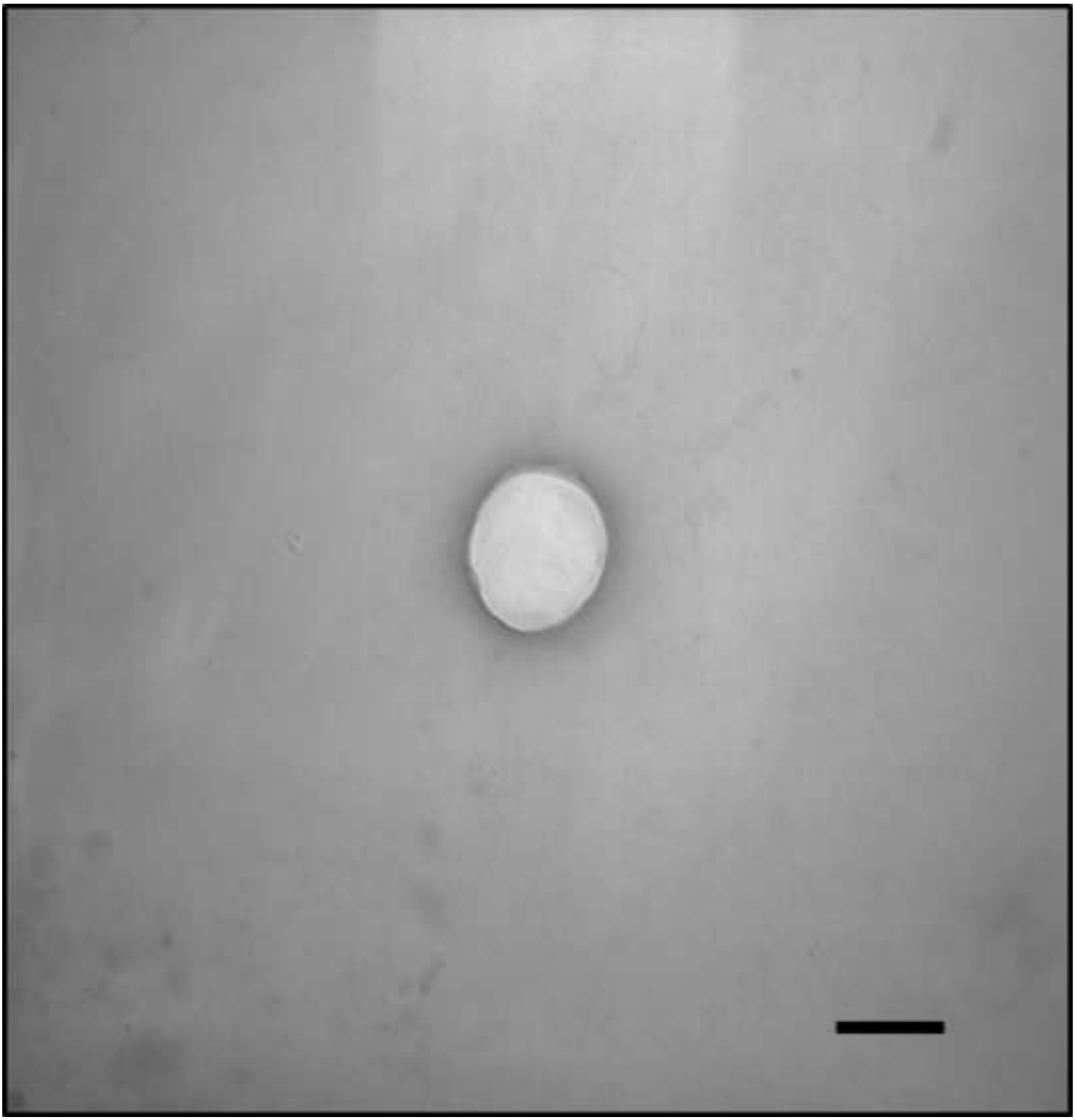

Figure 2

Click here to download Figure Figure 2.jpg

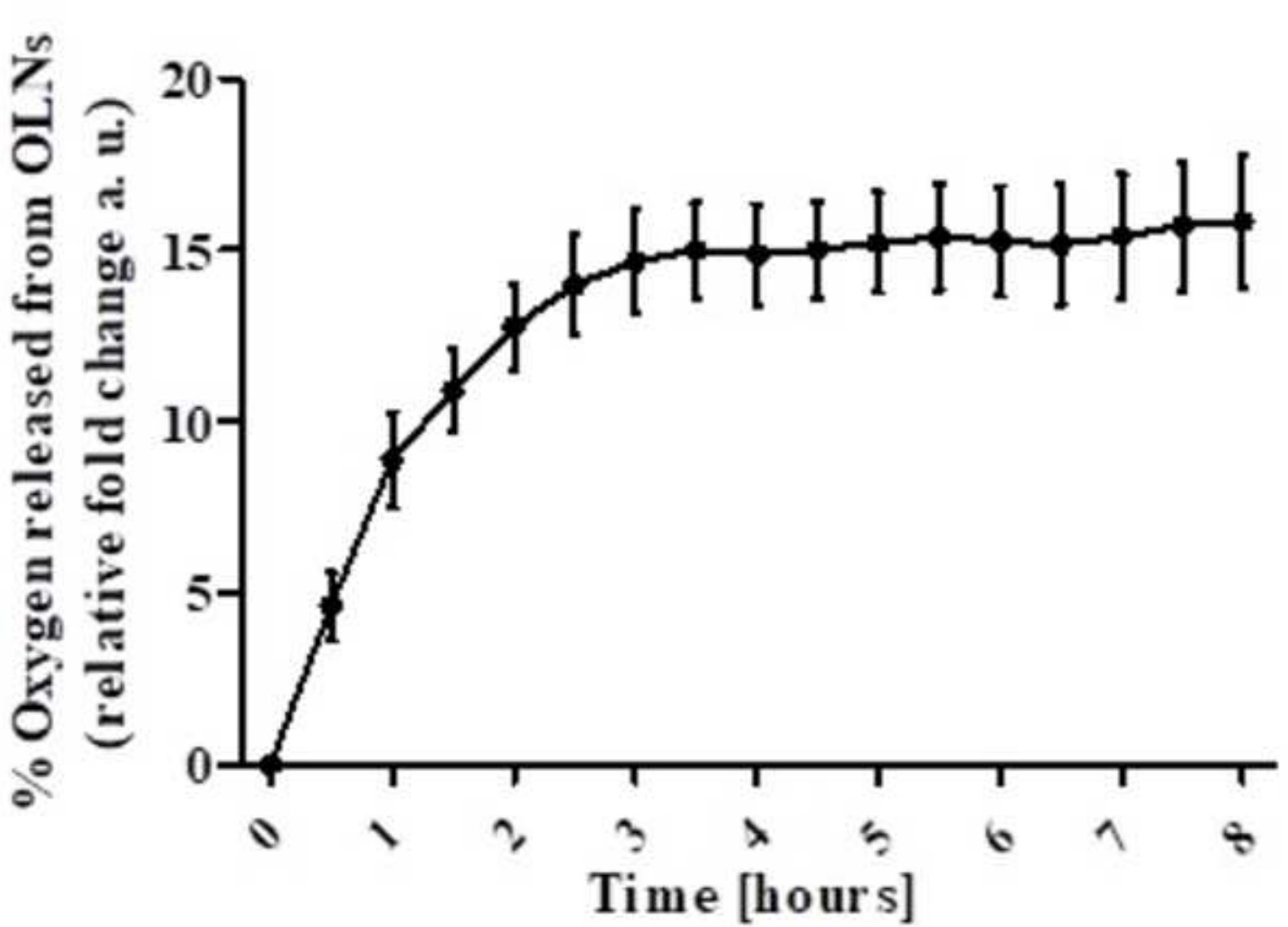

Figure 3

Click here to download Figure Figure 3.jpg

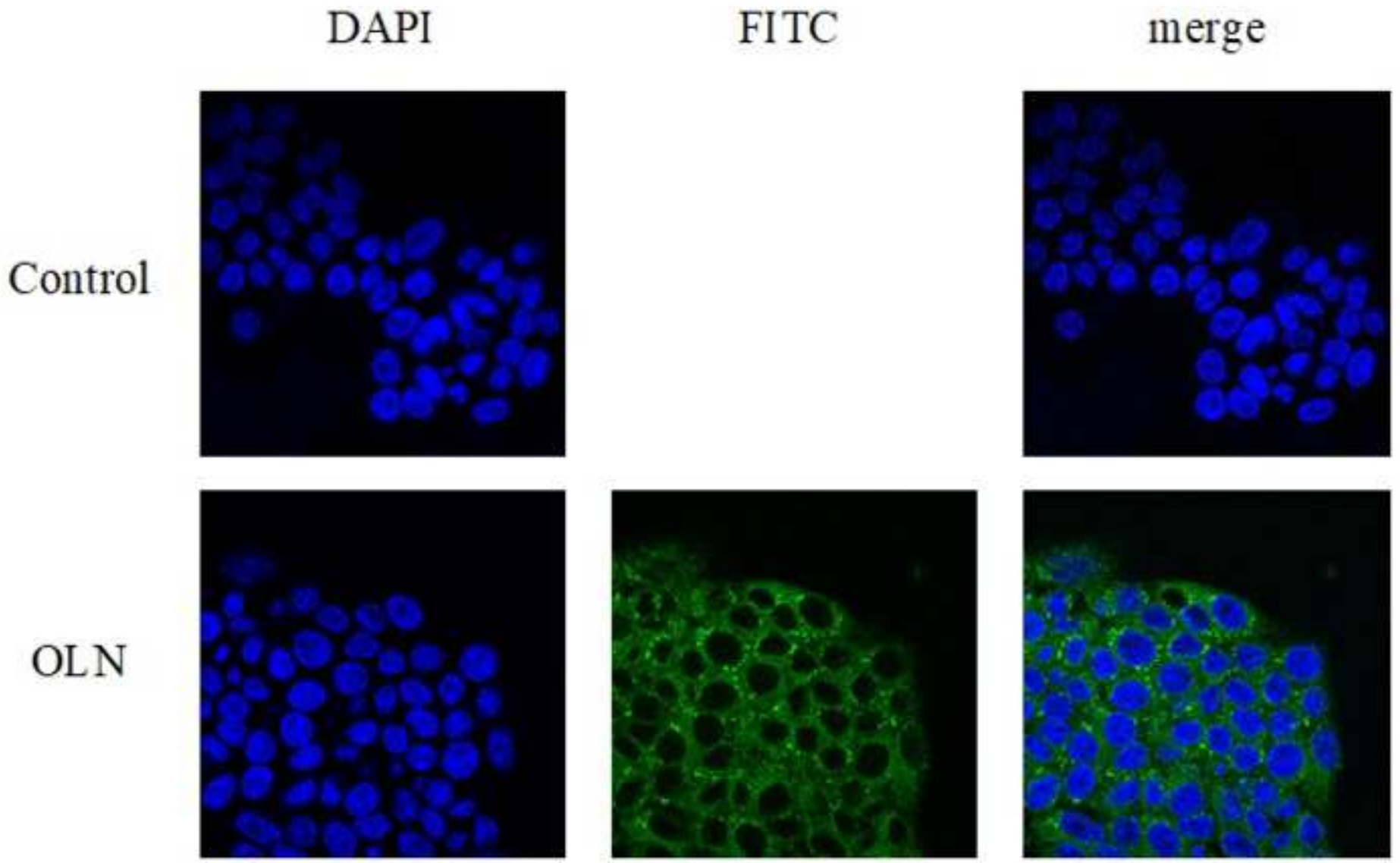

Figure 4



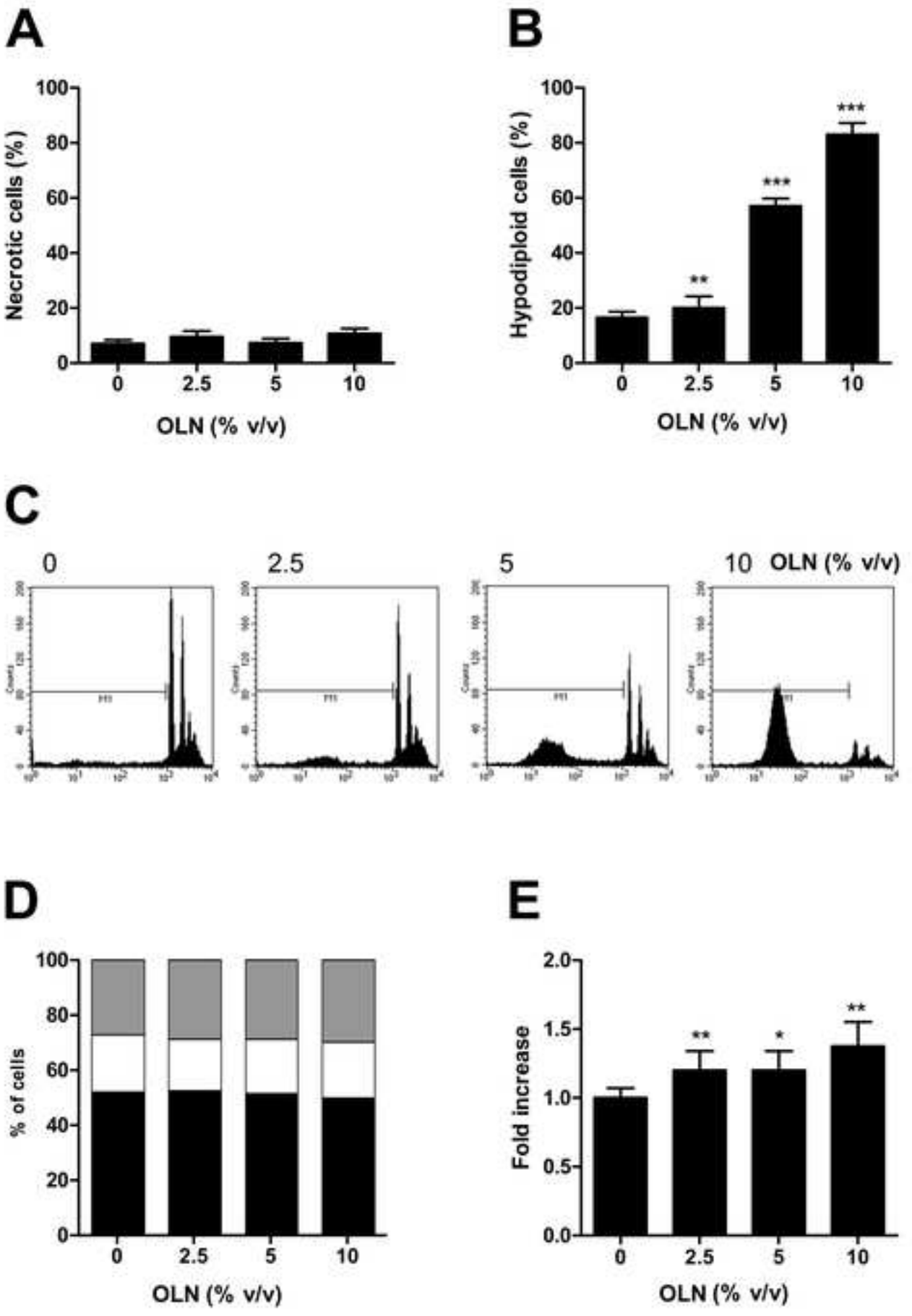

Figure 5

Click here to download Figure Figure 5.jpg

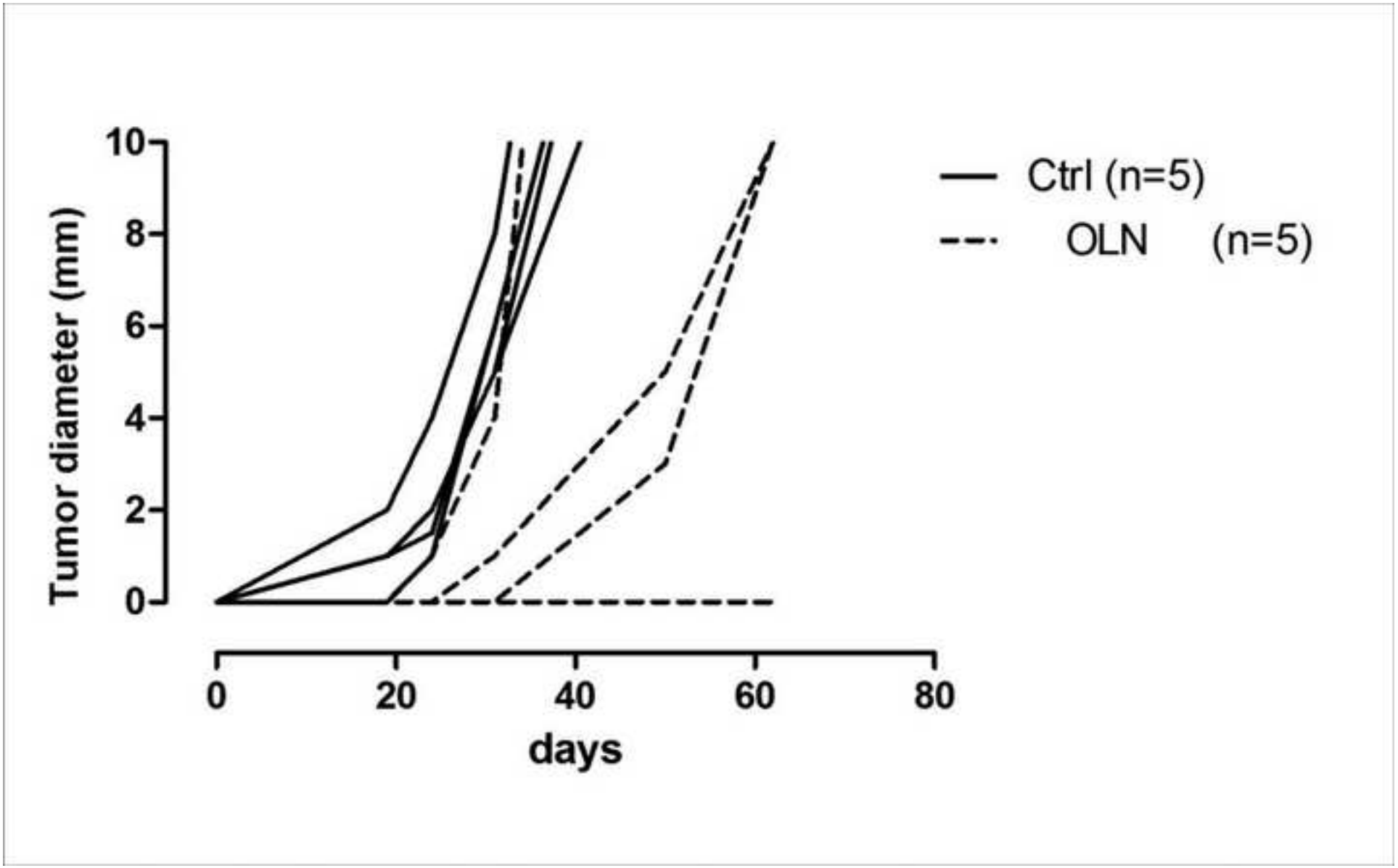

Figure 6

Click here to download Figure Figure 6.jpg

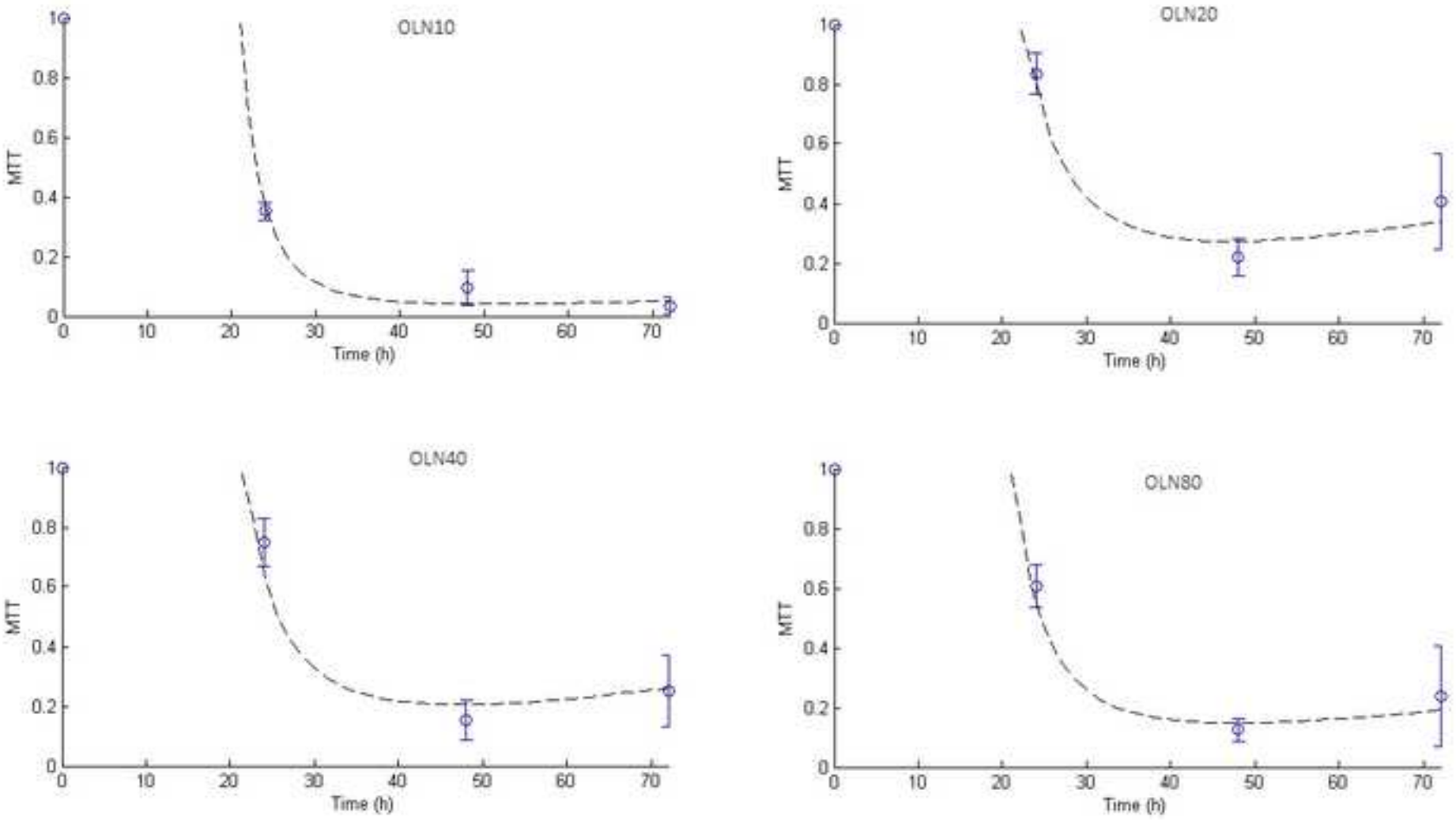

Figure 7

Click here to download Figure Figure 7.jpg